Arch Appl Mech (2011) 81:1427–1437
DOI 10.1007/s00419-010-0492-x

ORIGINAL

Alexey Kuznetsov · Musa Mammadov · Ibrahim Sultan · Eldar Hajilarov

Optimization of improved suspension system with inerter device of the quarter-car model in vibration analysis

Received: 28 June 2010 / Accepted: 23 November 2010 / Published online: 24 December 2010

Abstract In this paper, we analyze an improved suspension system with the incorporated inerter device of the quarter-car model to obtain optimal design parameters for maximum comfort level for a driver and passengers. That is achieved by finding the analytical solution for the system of ordinary differential equations, which enables us to generate an optimization problem whose objective function is based on the international standards of admissible acceleration levels (ISO 2631-1, Mechanical Vibration and Shock—Evaluation of Human Exposure to Whole-Body Vibration–Part 1, 1997). The considered approach ensures the highest level of comfort for the driver and passengers due to a favorable reduction in body vibrations. Numerical examples, based on actually measured road profiles, are presented at the end of the paper to prove the validity of the proposed approach and its suitability for the problem at hand.

Keywords Ride comfort · Vehicle suspension · Road profile variation · Multibody systems · Optimization

1 Introduction and literature review

The problem of finding optimal parameters of the vehicle suspension systems has been investigated by many researchers in the field of automotive engineering, e.g. [1] and [2]. The works presented in [3–8] feature good examples of efforts devoted to different methodologies of finding optimal parameters of suspensions with constant harmonic excitations. These papers utilize well-known numerical and finite element methods to obtain optimal parameters for designed models. On the other hand, [9] presents an outstanding input into the suspension problem by analyzing and optimizing vibrations of the two-mass quarter-car suspended by different types of linear elastic elements containing the innovative inerter device. The inerter characteristics and scheme design are presented in [9]: it is a simple rack-and-gear mechanism with a flywheel to reduce inertial forces caused by vibrations.

Our literature survey, thus far, suggests that the ISO standards on the evaluation of vibration accelerations [10] have not been utilized for the optimization procedure despite their great importance to the minimization of driver fatigue and the associated health hazards. Optimal results based on these standards would attain high levels of comfort, particularly, for long-term exposure to vertical accelerations. In this paper, we endeavor to address this current gap by formulating the optimization problem in terms of the ISO stipulated requirements. The mathematical nature of these requirements calls for innovative manipulation and builds up of

A. Kuznetsov (✉) · M. Mammadov · E. Hajilarov
Graduate School of Information Technology and Mathematical Sciences, University of Ballarat,
Mt. Helen Campus, Ballarat, VIC 3350, Australia
E-mail: alexeykuznetsov@students.ballarat.edu.au

I. Sultan
School of Science and Engineering, University of Ballarat, Mt. Helen Campus, Ballarat, VIC 3350, Australia

the optimization models as will be evident later in the paper. In this work, we use real road profiles for the optimization procedure that allows us to obtain credible results for the suspension problem.

We chose to employ the quarter-car model due to its being well understood in automotive engineering as suggested in [3] and [8]. For this model, an analytical closed-form solution will be obtained for the steady-state vibrations before an objective function is defined based on the ISO formulae. A search will then be conducted for the global minimum of the function with respect to the spring stiffness and the damping coefficient of the suspension damper. We then present several numerical examples at the end of the paper to demonstrate the validity of the approach and its suitability for the optimization of parameters of suspension system.

It is worthy of noting here that the main theme of this paper is the prevention of driver fatigue and associated health risks rather than a comprehensive dynamical study on the vehicle behavior on the road. In addition to the effects of lateral and vertical elasticity, such a study may require attention to the particulars of the kinematics and dynamics of both the suspension and steering linkages. This is beyond the scope of our current paper since it may divert effort and attention from the major objective.

This paper is structured in such a fashion that initially we introduce the problem and present the main stages of model development before numerical examples and results are discussed. Conclusions are then offered at the end of the paper.

2 Formulation of optimization problem

2.1 Quarter-car model based on Kelvin elements

In this paper, we consider a quarter-car model consisting of two Kelvin elements, where the upper mass M_2 represents the body of the vehicle and the lower mass M_1 is the unsprung mass of the wheel and other suspension parts. The principle concept of the quarter-car model is depicted in Fig. 1.

Herein, we construct an analytical solution for the case where a harmonic (vertical) deflection $u(t) = A\exp(i\omega t)$ is applied to the support of the lower mass M_1, where A is the amplitude of harmonic deflection of the support and ω is the circular frequency at which the deflection is applied. We shall also consider the gravity forces $M_1 g$ and $M_2 g$ of the corresponding masses. In the course of the analysis, we make the assumption that springs and dashpots used in this model are weightless and have linear time-independent characteristics. The governing second-order equations for the considered case are

$$\begin{cases} M_1\ddot{x}_1 + C_1\dot{x}_1 + K_1x_1 + B_2\left(\ddot{x}_1 - \ddot{x}_2\right) + C_2\left(\dot{x}_1 - \dot{x}_2\right) + K_2\left(x_1 - x_2\right) = C_1\dot{u}(t) + K_1u(t) - M_1g, \\ M_2\ddot{x}_2 + B_2\left(\ddot{x}_2 - \ddot{x}_1\right) + C_2\left(\dot{x}_2 - \dot{x}_1\right) + K_2\left(x_2 - x_1\right) = -M_2g \end{cases} \tag{1}$$

where x_1 and x_2 are deflections measured from the undisturbed state. In the above equations, C_1 and C_2 are the viscous damping coefficients, K_1 and K_2 are the spring rates, and B_2 is the "inertance" coefficient where all constants are independent of $x_1, x_2, \dot{x}_1, \dot{x}_2$, and time t.

The obvious general physical reasons imply

$$B_2 > 0, \quad M_q > 0, \quad C_q \geq 0, \quad K_q \geq 0, \quad q = 1, 2. \tag{2}$$

2.2 Deflection of the support and analytical solutions for quarter-car model

Introducing new variables $v_1 = \dot{x}_1$, $v_2 = \dot{x}_2$ and denoting $\vec{X} = (x_1, x_2, v_1, v_2)^T$, we can transform Eqs. (1) into the following system of four ODEs of the first order:

$$\dot{\vec{X}} = \mathbf{G}\cdot\vec{X} + \vec{P}_h(t) + \vec{P}_g(t), \tag{3}$$

where

$$\mathbf{G} = \begin{pmatrix} 0 & 0 & 1 & 0 \\ 0 & 0 & 0 & 1 \\ -\frac{M_2K_1+M_2K_2+B_2K_1}{D} & \frac{M_2K_2}{D} & -\frac{M_2C_1+M_2C_2+B_2C_1}{D} & \frac{M_2C_2}{D} \\ \frac{M_1K_2-B_2K_1}{D} & -\frac{M_1K_2}{D} & \frac{M_1C_2-B_2C_1}{D} & -\frac{M_1C_2}{D} \end{pmatrix}$$

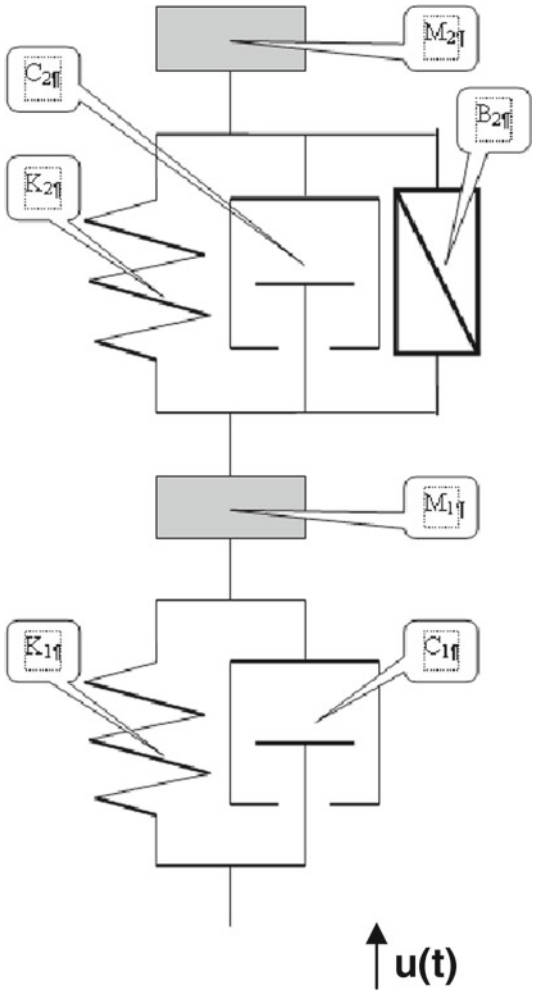

Fig. 1 Quarter-car model based on Kelvin elements and inerter device

$$\vec{P}_h(t) = \begin{pmatrix} 0 \\ 0 \\ \frac{M_2+B_2}{D}\left(C_1\dot{u}(t) + K_1u(t)\right) \\ \frac{B_2}{D}\left(C_1\dot{u}(t) + K_1u(t)\right) \end{pmatrix}; \quad \vec{P}_g(t) = \begin{pmatrix} 0 \\ 0 \\ -g \\ -g \end{pmatrix} \tag{4}$$
$$D = M_1M_2 + B_2\left(M_1 + M_2\right)$$

In (4), **G** is the system state matrix vector, loading vector $\vec{P}_h(t)$ is associated with the harmonic deflection, and vector $\vec{P}_g(t)$ corresponds to constant gravity forces of both masses.

Now, we derive analytical solution of (3). This solution can be expressed in the following form (see for example [11]):

$$\vec{X}(t) = (j\omega\mathbf{I} - \mathbf{G})^{-1} \cdot \left(\vec{P}_h(t) + \vec{P}_g(t)\right) \tag{5}$$

where $j = \sqrt{-1}$.

The solution of Eq. (5) for each of two masses in the case of harmonic and constant gravity deflections is as follows [11]:

$$\begin{cases} x_1(t) = D\left(K_2 - \omega^2\left(M_2 + B_2\right) + j\omega C_2\right)\frac{j\omega C_1+K_1}{d}A\exp(j\omega t) - g\frac{M_1+M_2}{K_1} \\ x_2(t) = D\left(K_2 - \omega^2 B_2 + j\omega C_2\right)\frac{j\omega C_1+K_1}{d}A\exp(j\omega t) - g\frac{M_1K_2+M_2K_2+M_2K_1}{K_1K_2} \end{cases} \tag{6}$$

Table 1 Principal frequency weighting coefficients for vertical direction accelerations of the standard ISO 2631 (1997)

Frequency band number	Frequency ω (Hz)	Principal frequency weightings W_i
−7	0.2	0.121
−6	0.25	0.182
…	…	…
0	1	0.482
1	1.25	0.484
2	1.6	0.494
…	…	…
7	5	1.039
8	6.3	1.054
9	8	1.036
…	…	…
19	80	0.132

where

$$\delta = D\left(\omega^4 D - j\omega^3\left(B_2C_1 + M_1C_2 + M_2C_1 + M_2C_2\right)\right.$$
$$\left. - \omega^2\left(M_2K_1 + M_1K_2 + B_2K_1 + M_2K_2 + C_1C_2\right) + j\omega\left(C_1K_2 + C_2K_1\right) + K_1K_2\right) \tag{7}$$

In obtained solutions (6), first two expressions on the right-hand side correspond to harmonic deflections and last term is the constant gravity deflection.

Taking the second derivative of (6), we can find the acceleration, $a_1(t)$ and $a_2(t)$, of the two systems masses as follows:

$$\begin{cases} a_1(t) = -\omega^2 D\left(K_2 - \omega^2\left(M_2 + B_2\right) + j\omega C_2\right)\frac{j\omega C_1 + K_1}{\delta} A\exp(j\omega t) \\ a_2(t) = -\omega^2 D\left(K_2 - \omega^2 B_2 + j\omega C_2\right)\frac{j\omega C_1 + K_1}{\delta} A\exp(j\omega t) \end{cases}. \tag{8}$$

Formula (8) can be used for evaluation of vertical accelerations at any fixed single frequency ω.

2.3 Vibration-based objective function

According to the ISO 2631 standards [10], vibration evaluation includes measurements of a weighted root-mean-square (r.m.s.) acceleration which we will denote as E. In general, the vibration spectrum consists of n independent bands with corresponding frequencies ω_i, where $i = 1, 2, \ldots, n$. According to the methodology provided by ISO, a weighting coefficient W_i, $i = 1, 2, \ldots, n$, should be applied to the acceleration associated with each frequency ω_i. The values of W_i as suggested by the ISO 2631 are given in Table 1.

The international code ISO 2631 defines the r.m.s. weighted acceleration E by the following formula:

$$E = \left(\frac{1}{T}\int_0^T b^2(t)dt\right)^{\frac{1}{2}} \tag{9}$$

where T is the duration of measurement and $b(t)$ is the frequency-weighted acceleration which is given as follows

$$b(t) = \left(\sum_{i=1}^{n}\left(W_i y_i(t)\right)^2\right)^{\frac{1}{2}} \tag{10}$$

where each steady-state vibration acceleration $y_i(t)$ is calculated in m/s^2, see [10].

Herein, our target is to find the spring constants and damper coefficients, which ensure the minimal value for the r.m.s. weighted acceleration E for the body of the vehicle. This leads to the following optimization problem

$$\text{Minimize: } F\left(K_1, K_2, C_1, C_2, B_2\right) = \left(\sum_i^n W_i^2 \frac{1}{T} \int_0^T y_i(t)^2 dt\right)^{\frac{1}{2}} \tag{11}$$

$$\text{Subject to : } K_1, K_2, C_1, C_2, B_2 \in \Delta \tag{12}$$

Herein, Δ represents the box constraint for the optimization parameters K_1, K_2, C_1, C_2, B_2.

2.4 Steady-state vibrations

In this paper, our focus is the steady-state part of the acceleration of the vehicle body associated with different frequencies $\omega_i, i = 1, \ldots, n$, that is

$$a_{2i}(t) = -\omega_i^2 D\left(K_2 - \omega_i^2 B_2 + j\omega_i C_2\right) \frac{j\omega_i C_1 + K_1}{\delta_i} A \exp(j\omega_i t).$$

The steady-state part of $a_{2i}(t)$ can be obtained by considering the real part of the acceleration of the upper mass and will be denoted by $y_i(t) = Re\left(a_{2i}(t)\right)$.

Therefore, to calculate r.m.s. weighted acceleration E (9) and the frequency-weighted acceleration $b(t)$ (10), we need to obtain the corresponding steady-state harmonic acceleration $y_i(t)$ of the upper mass associated with weighting coefficient W_i. So, first we introduce the integral (over some time interval T) of the squared real part of acceleration as follows:

$$S_i(T) = \frac{1}{T} \int_0^T y_i^2(t) dt = \frac{1}{T} \int_0^T \left(\alpha_i H_i + \beta_i L_i\right)^2 dt \tag{13}$$

where

$$\begin{aligned}
H_i &= \mathrm{A}_i \omega_i^2 \left(C_1 \omega_i \cos(\omega_i t) + K_1 \sin(\omega_i t)\right) \\
L_i &= \mathrm{A}_i \omega_i^2 \left(K_1 \cos(\omega_i t) - \omega_i C_1 \sin(\omega_i t)\right) \\
\alpha_i &= \frac{R_i \omega_i C_2 - Q_i K_2 + Q_i \omega_i^2 B_2}{(Q_i)^2 + (R_i)^2} \\
\beta_i &= \frac{R_i \omega_i^2 B_2 - Q_i \omega_i C_2 - R_i K_2}{(Q_i)^2 + (R_i)^2} \\
Q_i &= \omega_i \left(C_1 K_2 + C_2 K_1 - \omega_i^2 \left(C_1 M_2 + C_2 M_1 + C_2 M_2 + B_2 C_1\right)\right) \\
R_i &= K_1 K_2 - \omega_i^2 \left(C_1 C_2 + K_1 M_2 + K_2 M_1 + K_2 M_2 + B_2 K_1\right) + \omega_i^4 D
\end{aligned} \tag{14}$$

After some transformations, the integral in (13) can be represented in the following form:

$$S_i(T) = A_i^2 \omega_i^4 \left[U_i \left(\frac{1}{2} - \frac{\sin(2\omega_i T)}{4T\omega_i}\right) + V_i \left(\frac{-\cos(2\omega_i T)}{4T\omega_i}\right) + X_i \left(\frac{1}{2} + \frac{\sin(2\omega_i T)}{4T\omega_i}\right)\right] \tag{15}$$

where

$$\begin{aligned}
U_i &= \left(\alpha_i K_1 + \beta_i \omega_i C_1\right)^2 \\
V_i &= \alpha_i^2 \omega_i K_1 C_1 + \alpha_i \beta_i K_1^2 - \alpha_i \beta_i \omega_i^2 C_1^2 - \beta_i^2 \omega_i K_1 C \\
X_i &= \left(\alpha_i \omega_i C_1 + \beta_i K_1\right)^2
\end{aligned} \tag{16}$$

It can be observed that the terms in Eq. (15) associated with $\frac{\sin(2\omega_i T)}{T}$ and $\frac{\cos(2\omega_i T)}{T}$ will tend to zero when considering large time periods of driving, i.e. at $T \to \infty$. Taking the time limit in (15) yields

$$\tilde{S}_i \equiv \lim_{T\to\infty} S_i(T) = \frac{\omega_i^4 \mathrm{A}_i^2 \left(\omega_i^2 C_1^2 + K_1^2\right)\left(\omega_i^2 C_2^2 + \left(K_2 - \omega_i^2 B_2\right)^2\right)}{2\left(R_i^2 + Q_i^2\right)} \tag{17}$$

Thus, for large time periods, the objective function (11) can be approximated by replacing $S_i(T)$ with its time limit $\tilde{S}_i$ yielding:

$$\tilde{F}\left(K_1, K_2, C_1, C_2, B_2\right) = \left(\sum_i^n \tilde{S}_i W_i^2\right)^{\frac{1}{2}}, \tag{18}$$

where n is the number of band frequencies present in the vibration spectrum.

Therefore, we obtain the following optimization problem:

$$\text{Minimize: } \tilde{F}\left(K_1, K_2, C_1, C_2, B_2\right) \tag{19}$$

$$\text{Subject to : } K_1, K_2, C_1, C_2, B_2 \in \Delta \tag{20}$$

In contrast to (11), (12), problem (19), (20) involves steady-state solutions only and does not depend on the duration of measurement T. Note that this is very important as it can provide an optimal solution $\left(K_1^*, K_2^*, C_1^*, C_2^*, B_2^*\right)$ for the parameters of the car suspension system that does not depend on the measurement time T. On the other hand, problem (19), (20) is an approximation of problem (11), (12) when $T \to \infty$, that is, this optimal solution can be interpret as an "almost" optimal solution to (11), (12) as well for large duration periods of measurements.

Problem (19), (20) is a highly nonlinear optimization problem having many local optimal solutions. That is why, we need to apply global optimization algorithms to find a global optimal solution to (19), (20). In the numerical experiments below, we will use the Algorithm for Global Optimization Problems (AGOP), introduced in [12]. This global optimization algorithm is designed for solving continuous optimization problems with defined box constraints. The efficiency of the algorithm has been demonstrated in solving many difficult practical problems (see [13] and references therein).

3 Numerical examples

Herein, we perform Power Spectral Density calculations of three sections of rural roads for typical speed limits that range from 60 to 100 km/h. In this paper, we used road profiles of the following roads: Alfred street, Wendouree Parade street, and Ring Road, Ballarat, Victoria, Australia. Road profiles data were provided by the School of Science and Engineering, University of Ballarat. (Fig. 2)

Considering vibration spectra of the given road profiles, we used frequencies ω_i from the range 0.2–80 Hz, which are associated with weighting values W_i more than 0.1 as per the ISO 2631, see Table 1. This allowed us to avoid a number of specific frequencies with minor influence on the ride comfort level. The values of various quarter-car model parameters are taken in reference to [14]. In many publications, for example [1] and [15], the tire of the wheel is considered as a structure with no damping properties, i.e. $C_1 = 0$. Particularly, in [15], it is stated that a typical pressured tire exhibits negligible damping values, and it can be considered as a component of the wheel with stiffness only. Therefore, in the numerical examples when solving problem (19), (20), this parameter is fixed by setting $C_1 = 0$ that neglects damping properties of the tire.

Also, we consider several scenarios to evaluate the influence of the mass of the vehicle body on comfort level. Therefore, fixing $M_1 = 20$ kg we define three mass ratios $\frac{M_2}{M_1} = [15; 20; 25]$. The domains assumed for the springs constants are given as $K_1 \in [180000, 240000]$(N/m), $K_2 \in [10000, 25000]$(N/m), the coefficient of the damper is given as $C_2 \in [2000, 4000]$(N sec /m), $B_2 \in [0, 4]$(kg). The minimum value of the spring stiffness, K_1, corresponds to a low pressure tire (24 psi), and the maximum value corresponds to an over-inflated tyre (44 psi). The limiting values imposed on the constants of spring K_2, damper C_2, and inerter B_2 are determined from the engineering point of view of suspension deflection using [14] as reference. Thus, we can represent a constrain box as $\Delta = [180000, 240000], [10000, 25000], [2000, 4000], [0, 4]$.

Performing optimization procedure using AGOP software and finding global solution, we can find optimal parameters of the tire stiffness K_1, suspension spring K_2, damper C_2, and inerter to achieve minimum values

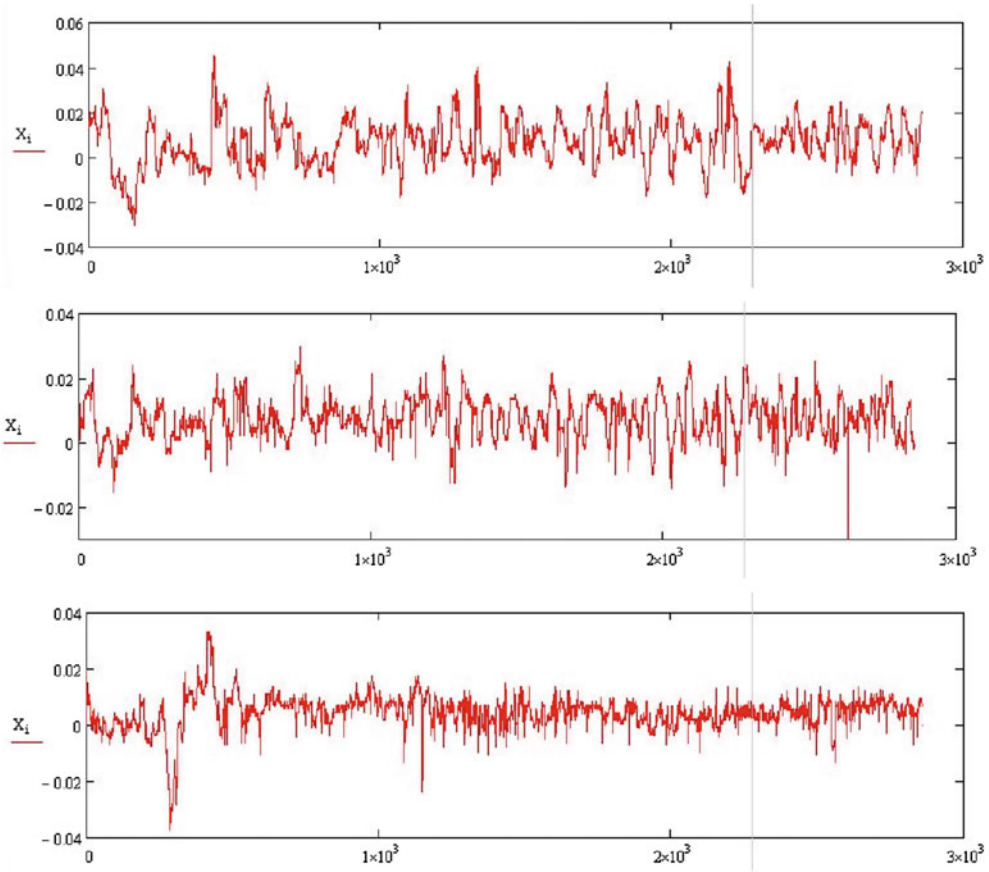

Fig. 2 Measured road profiles of Alfred street (*top curve*), Wendouree Parade street (*middle curve*), and Ring Road (*bottom curve*). *Vertical axes* show unevenness amplitudes, *horizontal axes* show number of points in road profile (length of the measured profiles are equal to 100 m)

Table 2 The optimal parameter values C_2, K_2 and B_2 of suspension and tyre stiffness K_1 of the quarter-car model for the considered sections of roads

Vehicle speed range (km/h)	Optimal values of the parameters	Alfred street	Wendouree Parade street	Ring Road
60–100	K_1 (N/m)	180000		
	K_2 (N/m)	10000		
	C_2 (N s/m)	2000		
60	B_2 (kg)	0.512	0.524	0.395
65		0	0	0
70		0	0	0
75		0	0	0.524
80		0.861	0	0.558
85		0.951	0	0
90		0.425	0	0.145
95		0	0	0.548
100		1.171	0	0.403

of the objective function of the upper mass of the quarter-car model on the considered roads of the city of Ballarat. Optimal values found of the parameters K_1, K_2, C_2 and B_2 for all three mass ratios are given in Table 2.

In Fig. 3, we listed minimum values of objective function $\left(\mathrm{m/s^2}\right)$ which correspond to the optimal parameters of the inerter B_2, damper C_2, suspension spring K_2, and tire stiffness K_1 of the quarter-car model for the analyzed mass ratios $\frac{M_2}{M_1}$.

According to the code presented in the ISO 2631, the criterion employed to evaluate the intensity of vibration transmitted to a human is based on the length of time (in hours) over which exposure to vibration results

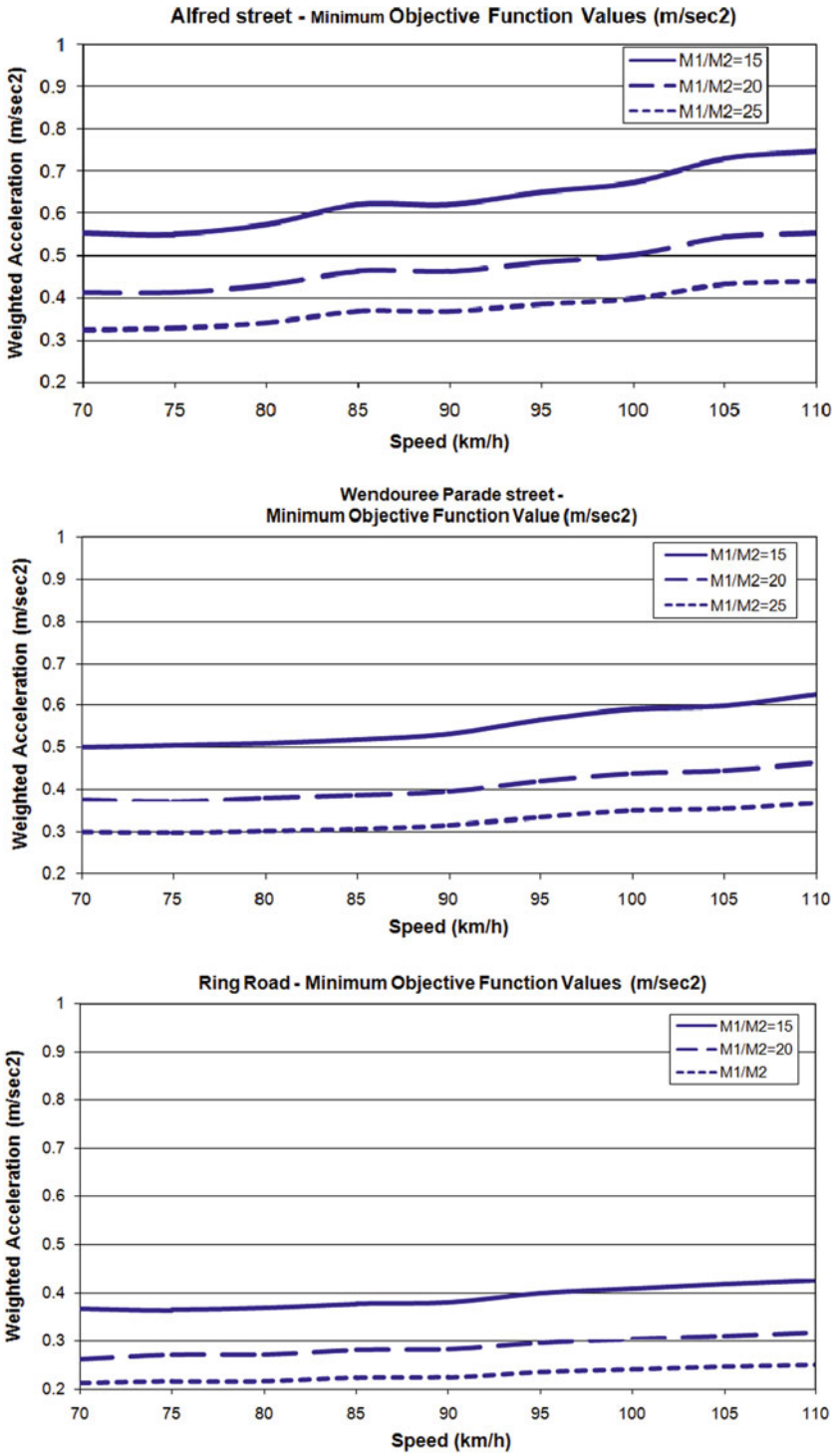

Fig. 3 The minimum values of objective function (m/s^2) corresponding to optimal parameters of the inerter B_2, damper C_2, spring of suspension K_2, and tire stiffness K_1 of the quarter-car model on Ballarat roads for the considered mass ratios $\frac{M_2}{M_1}$

in no health risks (NH), potential health risks (PR) or likely health risks (HR). For better presentation, the ISO curves which define these three levels of vibration exposure are shown in Fig. 4.

In Table 3, we represent vibration exposure in the NH, PR, and HR criteria for one scenario $\frac{M_2}{M_1} = 15$ (Fig. 3) using ISO chart shown in Fig. 4.

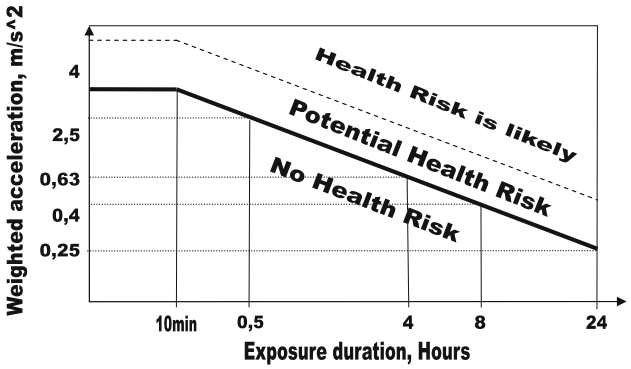

Fig. 4 Maximum vibration exposure time (hours) that corresponds to No Health Risk condition, Potential Health Risk, and Health Risk is likely in accordance with ISO2631

Table 3 Health guidance caution zones (B2) of ISO 2631-1: time limits (hours) of vibration exposure with No Health Risk conditions (NH), Potential Risk conditions (PR), and Health Risk conditions (HR) for the scenario when $\frac{M_2}{M_1} = 15$

Vehicle speed (km/h)	Alfred street			Wendouree Parade street			Ring Road		
	NH	PR	HR	NH	PR	HR	NH	PR	HR
60	6	6–17	17–24	7	7–18	18–24	12	10–24	24
65	6	6–17	17–24	7	7–28	18–24	12	10–24	24
70	6	6–17	17–24	7	7–28	18–24	12	10–24	24
75	5	5–14	14–24	7	7–28	18–24	12	10–24	24
80	5	5–14	14–24	7	7–18	18–24	12	10–24	24
85	4	4–12	12–24	6	6–18	18–24	11	11–24	24
90	4	4–12	12–24	5	5–14	14–24	11	11–24	24
95	3	3–11	11–24	5	5–14	14–24	11	11–24	24
100	3	3–11	11–24	5	5–14	14–24	11	11–24	24

The results in Table 2 reveal some tendencies and suggest some conclusions. For example, to achieve the best comfort performance in vehicle on rural roads, the tires should have minimal stiffness, as parameter K_1 remains at minimum in all the considered cases. On the other hand, suspension systems require minimal stiffness of the spring K_2 as the damping coefficient C_2 remains at the lowest values of the defined box Δ. Also, inerter B_2 should have values closed to the lowest boundary of the box Δ to provide minimum values of the objective function. So, it means that any speed on rural roads requires the softest suspension settings for improved comfort level.

At the same time, the results presented in Fig. 3 show that heavier body of the vehicle leads to the lower accelerations and provides higher comfort level. This fact can be easily investigated analytically analyzing formula (17) and (14).

From an engineering point of view, it is very important to observe the influence of each parameter on the comfort level. Figure 5 shows the influence of the tire stiffness, suspension spring stiffness, damping coefficient, and the inerter mass on the comfort level. To evaluate influence of each parameter on comfort level, we used as a reference Alfred Street road profile at a driving speed of 60 km/h in the case when mass ratio $\frac{M_2}{M_1} = 15$. In particular, on the top plot, we can see the influence of the tire stiffness, K_1, on the comfort level, while the parameters K_2, C_2 and B_2 are fixed at minimum values within box Δ. The second plot shows the influence of suspension spring stiffness, K_2, on the comfort level, when other three parameters K_1, C_2 and B_2 remain at the lowest boundaries of the considered box Δ. The third plot depicts the influence of the damping coefficient C_2 on the comfort level, with parameters K_1, K_2 and B_2 fixed at their minimum values within the considered boundaries. The bottom plot reflects the influence of the inerter coefficient B_2 on the comfort level, while other parameters K_1, K_2 and C_2 remain at the lowest boundaries.

Figure 5 reveals that for any driving speed, on rural roads, the stiffness of the tires, and mass of the inerter of the suspension system do not affect the comfort level of the vehicle as much as the stiffness of the suspension springs do. On the other hand, the comfort level is very sensitive to the viscous damping coefficients. These results generally agree with the concepts suggested in [15].

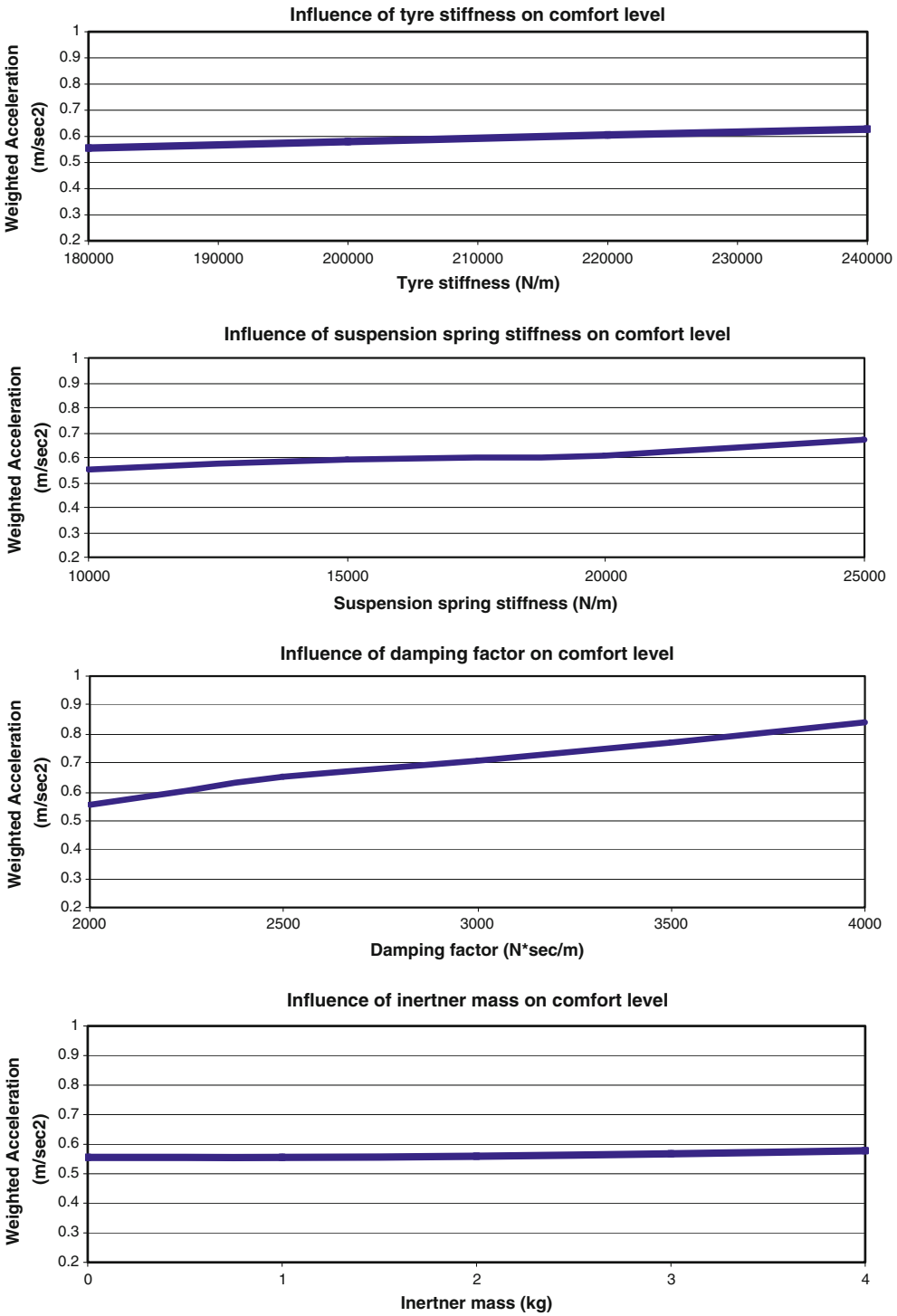

Fig. 5 Influence of tyre stiffness, stiffness of the suspension spring, damping factor, and inerter mass on objective function values (ISO 2631 weighted accelerations)

4 Conclusions

This paper presents a contribution to vibration analysis in automotive engineering by evaluating the vibration transmitted from road profile variations to a driver or a passenger of a vehicle. A mathematical model is

constructed and manipulated to calculate the steady-state component of the transmitted vibration. This model is then optimized, in reference to the standard ISO 2631, to obtain suitable values for the suspension system parameters. Numerical results reveal information on how different parameters affect the comfort level of a road vehicle. The considered model is suitable for vibration analysis and optimization of vehicle suspension system.

References

1. Chen, P.C., Huang, A.C.: Adaptive multi-surface sliding control of hydraulic active suspension systems. J. Vib. Control **11** (2005)
2. Harris, C.M., Piersol, A.G. (eds.): Harris' Shock and Vibration Handbook, 5th edn. McGraw-Hill, NY (2002)
3. Georgiou, G., Verros, G., Natsiavas, S.: Multi-objective optimization of quarter-car models with a passive or semi-active suspension system. Veh. Syst. Dyn. **45**(1), 77–92 (2007)
4. Metallidis, P., Verros, G., Natsiavas, S.: Fault detection and optimal sensor location in vehicle suspensions. J. Vib. Control **9** (2003)
5. Papalukopoulos, C., Giadopulos, D., Natsiavas, S.: Dynamics of large scale vehicle models coupled with driver biodynamic models. In: 5th GRACM International Congress on Computational Mechanics. Limassol (2005)
6. Papalukopoulos, C., Theodosiou, C., Natsiavas, S.: Nonlinear dynamics of vehicle models coupled with biodynamic passenger models. In: 2nd International Conference on Nonlinear Normal Modes and Localization in Vibrating Systems. Samos (2006)
7. Verros, G., Goudas, H., Natsiavas, S.: Dynamics of large scale vehicle models using ADAMS/FLEX. In: International ADAMS User Conference (2000)
8. Verros, G., Nastiavas, S., Papadimitriou, C.: Design optimization of quarter-car models with passive and semi-active suspensions under random road excitation. J. Vib. Control **1**, 581–606 (2005)
9. Scheibe, F., Smith, M.: Analytical solutions for optimal ride comfort and tyre grip for passive vehicle suspensions. J. Veh. Syst. Dyn. **47**, 1229–1252 (2009)
10. ISO 2631-1: Mechanical Vibration and Shock—Evaluation of Human Exposure to Whole-Body Vibration–Part 1. (1997)
11. Zwillinger, D.: Handbook of Differential Equations, 3rd edn. Academic Press, NY (1997)
12. Mammadov, M.A.: A new global optimization algorithm based on dynamical systems approach. In: Rubinov, A., Sniedovich, M. (eds.) 6th International Conference on Optimization: Techniques and Applications. Ballarat, Australia (2004)
13. Tilakaratne, C.D., Mammadov M.A., Morris, S.A.: Modified neural network algorithms for predicting trading signals of stock market indices. J. Appl. Mathe. Decis. Sci. **2009**, 22 (2009), Article ID 125308. doi:10.1155/2009/125308
14. Werner, S.: White noise excitation of road vehicle structures. Sadhana **31**(Part 4), 487–503 (2007)
15. Khachaturov, A.: Dynamics of the System Road-Tyre-Vehicle-Driver (in Russian). Moscow (1976)